

Chapter 11

Mechanical Properties: Fast Fracture

*The careful text-books measure
(Let all who build beware!)
The load, the shock, the pressure
Material can bear.
So when the buckled girder
Lets down the grinding span.
The blame of loss, or murder,
Is laid upon the man.
Not on the stuff — the Man!*

R. Kipling, “*Hymn of the Breaking Strain*”

11.1 Introduction

Sometime before the dawn of civilization, some hominid discovered that the edge of a broken stone was quite useful for killing prey and warding off predators. This seminal juncture in human history has been recognized by archeologists who refer to it as the stone age. C. Smith¹⁷⁸ goes further by stating, “Man probably owes his very existence to a basic property of inorganic matter, the brittleness of certain ionic compounds.” In this context, Kipling’s hymn and J. E. Gordon’s statement¹⁷⁹ that “The worst sin in an engineering material is not lack of strength or lack of stiffness, desirable as these properties are, but lack of toughness, that is to say, lack of resistance to the propagation of cracks” stand in sharp contrast. But it is this contrast that in a very real sense summarizes the short history of technical ceramics: what was good enough for millennia now falls short. After all, the consequences of a broken mirror are not as dire as those of, say, an exploding turbine blade. It could be argued, with some justification, that were it not for their brittleness, the use of ceramics for structural applications, especially

¹⁷⁸ C. S. Smith, *Science*, **148**:908 (1965).

¹⁷⁹ J. E. Gordon, *The New Science of Engineering Materials*, 2d ed., Princeton University Press, Princeton, New Jersey, 1976.

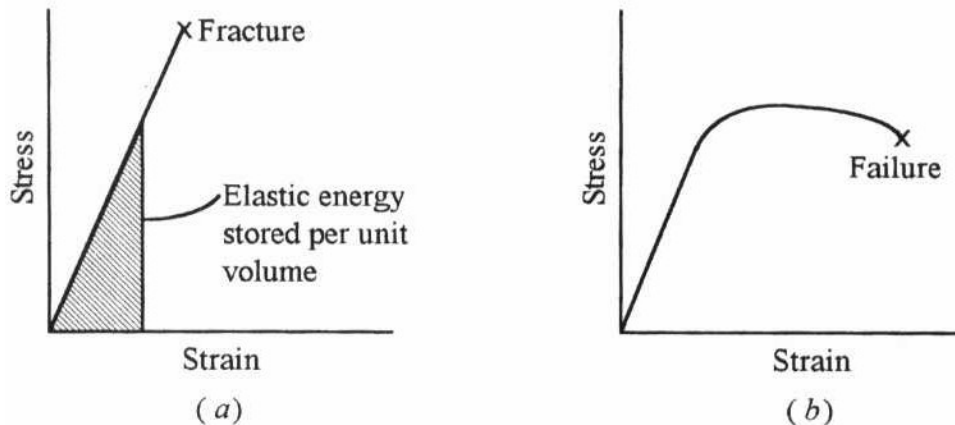


Figure 11.1 Typical stress–strain curves for (a) brittle solids and (b) ductile materials.

at elevated temperatures, would be much more widespread since they possess other very attractive properties such as hardness, stiffness, and oxidation and creep resistance.

As should be familiar to most, the application of a stress to any solid will initially result in a reversible elastic strain that is followed by either fracture without much plastic deformation (Fig. 11.1a) or fracture that is preceded by plastic deformation (Fig. 11.1b). Ceramics and glasses fall in the former category and are thus considered brittle solids, whereas most metals and polymers above their glass transition temperature fall into the latter category.

The theoretical stress level at which a material is expected to fracture by bond rupture was discussed in Chap. 4 and estimated to be on the order of $Y/10$, where Y is Young's modulus. Given that Y for ceramics (see Table 11.1) ranges between 100 and 500 GPa, the expected “ideal” fracture stress is quite high — on the order of 10 to 50 GPa. For reasons that will become apparent shortly, the presence of flaws, such as shown in Fig. 11.2, in brittle solids will greatly reduce the stress at which they fail. Conversely, it is well established that extraordinary strengths can be achieved if they are flaw-free. For example, a defect-free silica glass rod can be elastically deformed to stresses that exceed 5 GPa! Thus it may be concluded, correctly one might add, that certain flaws within a material serve to promote fracture at stress levels that are well below the ideal fracture stress.

The stochastic nature of flaws present in brittle solids together with the flaw sensitivity of the latter has important design ramifications as well. Strength variations of ± 25 percent from the mean are not uncommon and are quite large when compared to, say, the spread of flow stresses in metals, which are typically within just a few percent. Needless to say, such variability, together with the sudden nature of brittle failure, poses a veritable challenge for design engineers considering using ceramics for structural and other critical applications.

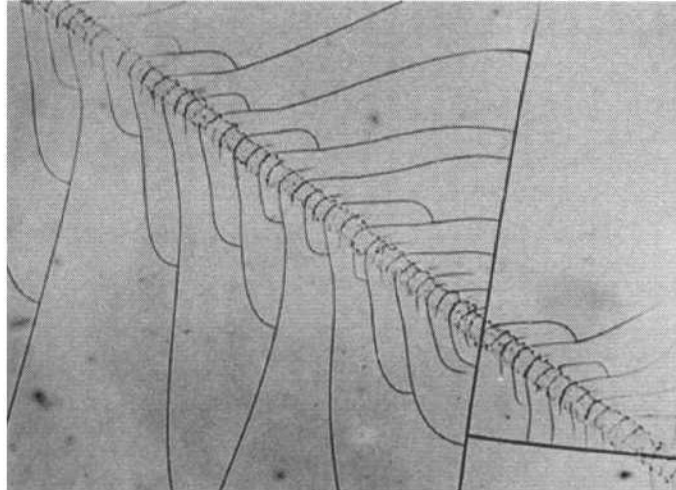


Figure 11.2 Surface cracks caused by the accidental contact of a glass surface with dust particles or another solid surface can result in significant reductions in strength.

Flaws, their shape, and their propagation are the central themes of this chapter. The various aspects of brittle failure are discussed from several viewpoints. The concepts of fracture toughness and flaw sensitivity are discussed first. The factors influencing the strengths of ceramics are dealt with in Sec. 11.3.¹⁸⁰ Toughening mechanisms are dealt with in Sec. 11.4. Section 11.5 introduces the statistics of brittle failure and a methodology for design.

11.2 Fracture Toughness

11.2.1 Flaw Sensitivity

To illustrate what is meant by flaw or notch sensitivity, consider the schematic of what occurs at the base of an atomically sharp crack upon the application of a load F_{app} . For a crack-free sample (Fig. 11.3a), each chain of atoms will carry its share of the load F/n , where n is the number of chains, i.e., the applied stress σ_{app} is said to be uniformly distributed. The introduction of a surface crack results in a stress redistribution such that the load that was supported by the severed bonds is now being carried by only a few bonds at the crack tip (Fig. 11.3b). Said otherwise, the presence of a flaw will *locally amplify the applied stress at the crack tip* σ_{tip} . As σ_{app} is increased, σ_{tip} increases accordingly and moves up the stress versus interatomic distance curve, as shown in Fig. 11.3c. As long as $\sigma_{\text{tip}} < \sigma_{\text{max}}$, the situation is stable and the flaw will not propagate. However, if at any time σ_{tip} exceeds σ_{max} , the situation becomes catastrophically unstable (not

¹⁸⁰ The time-dependent mechanical properties such as creep and subcritical crack growth are dealt with separately in the next chapter.

unlike the bursting of a dam). Based on this simple picture, the reason why brittle fracture occurs rapidly and without warning, with cracks propagating at velocities approaching the speed of sound, should now be obvious. Furthermore, it should also be obvious why ceramics are much stronger in compression than in tension.

To be a little more quantitative in predicting the applied stress that would lead to failure, σ_{tip} would have to be calculated and equated to σ_{max}

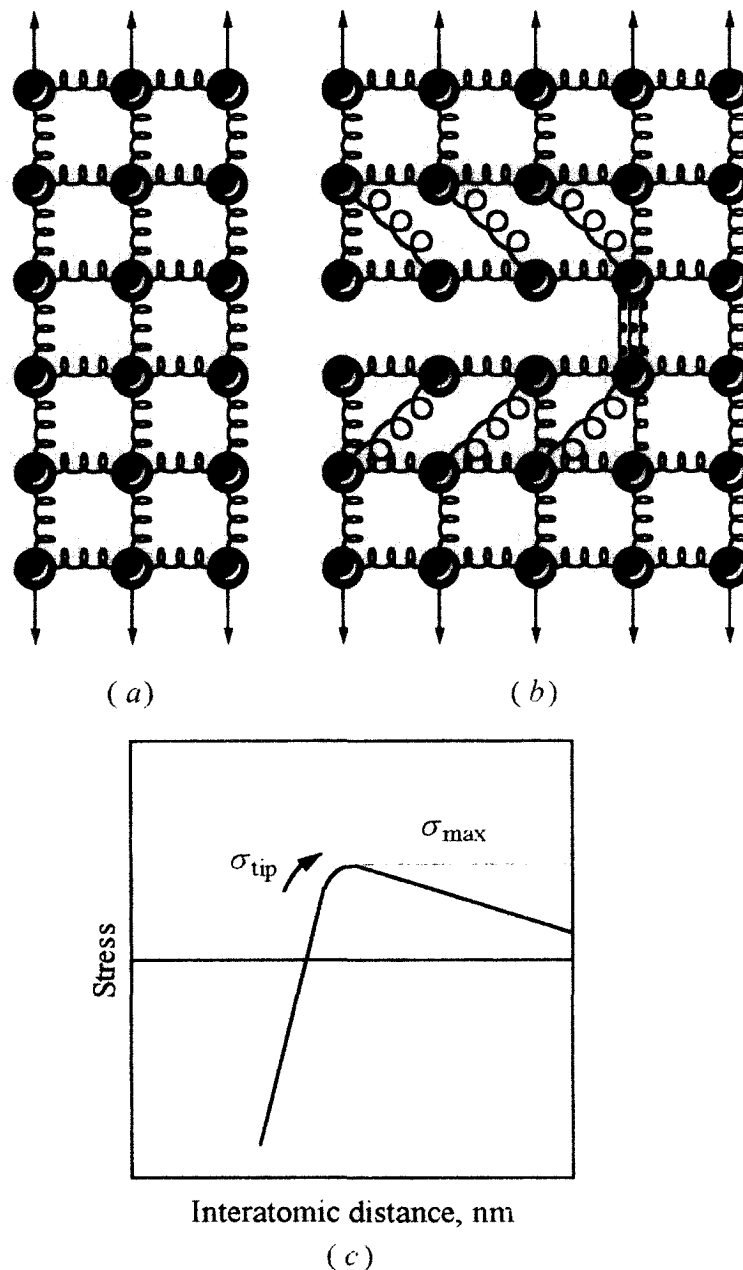


Figure 11.3 (a) Depiction of a uniform stress. (b) Stress redistribution as a result of the presence of a crack. (c) For a given applied load, as the crack grows and the bonds are sequentially ruptured, σ_{tip} moves up the stress versus displacement curve toward σ_{max} . When $\sigma_{\text{tip}} \approx \sigma_{\text{max}}$, catastrophic failure occurs. Note that this figure is identical to Fig. 4.6, except that here the y axis represents the stress on the bond rather than the applied force.

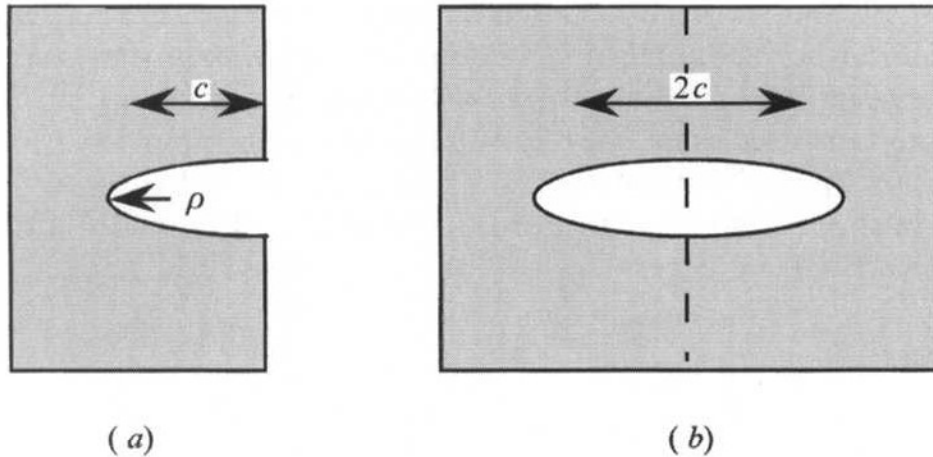


Figure 11.4 (a) Surface crack of length c and radius of curvature ρ . (b) Interior crack of length $2c$. Note that from a fracture point of view, they are equivalent.

or $Y/10$. Calculating σ_{tip} is rather complicated (only the final result is given here) and is a function of the type of loading, sample, crack geometry, etc.¹⁸¹ However, for a thin sheet, it can be shown that σ_{tip} is related to the applied stress by

$$\sigma_{\text{tip}} = 2\sigma_{\text{app}} \sqrt{\frac{c}{\rho}} \quad (11.1)$$

where c and ρ are, respectively, the crack length and its radius of curvature¹⁸² (Fig. 11.4).

Since, as noted above, fracture can be reasonably assumed to occur when $\sigma_{\text{tip}} = \sigma_{\text{max}} \approx Y/10$, it follows that

$$\sigma_f \approx \frac{Y}{20} \sqrt{\frac{\rho}{c}} \quad (11.2)$$

where σ_f is the stress at fracture. This equation predicts that (1) σ_f is inversely proportional to the square root of the flaw size and (2) sharp cracks, i.e., those with a small ρ , are more deleterious than blunt cracks. Both predictions are in good agreement with numerous experimental observations.

11.2.2 Energy Criteria for Fracture — The Griffith Criterion

An alternate and ultimately more versatile approach to the problem of fracture was developed in the early 1920s by Griffith.¹⁸³ His basic idea was

¹⁸¹ C. E. Inglis, *Trans. Inst. Naval Archit.*, **55**:219 (1913).

¹⁸² This equation strictly applies to a surface crack of length c , or an interior crack of length $2c$ in a thin sheet. Since the surface of the material cannot support a stress normal to it, this condition corresponds to the plane stress condition (the stress is two-dimensional). In thick components, the situation is more complicated, but for brittle materials the two expressions vary slightly.

¹⁸³ A. A. Griffith, *Phil. Trans. R. Acad.*, **A221**:163 (1920).

to balance the energy consumed in forming new surface as a crack propagates against the elastic energy released. The critical condition for fracture, then, occurs when the rate at which energy is released is greater than the rate at which it is consumed. The approach taken here is a simplified version of the original approach, and it entails deriving an expression for the energy changes resulting from the introduction of a flaw of length c in a material subjected to a uniform stress σ_{app} .

Strain energy

When a solid is uniformly elastically stressed, all bonds in the material elongate and the work done by the applied stress is converted to elastic energy that is stored in the stretched bonds. The magnitude of the elastic energy stored per unit volume is given by the area under the stress-strain curve¹⁸⁴ (Fig. 11.1a), or

$$U_{\text{elas}} = \frac{1}{2} \varepsilon \sigma_{\text{app}} = \frac{1}{2} \frac{\sigma_{\text{app}}^2}{Y} \quad (11.3)$$

The total energy of the parallelepiped of volume V_0 subjected to a uniform stress σ_{app} (Fig. 11.5a) increases to

$$U = U_0 + V_0 U_{\text{elas}} = U_0 + \frac{V_0 \sigma_{\text{app}}^2}{2Y} \quad (11.4)$$

where U_0 its free energy in the absence of stress.

In the presence of a surface crack of length c (Fig. 11.5b), it is fair to assume that some volume around that crack will relax (i.e., the bonds in that volume will relax and lose their strain energy). Assuming — it is not a bad assumption, as will become clear shortly — that the relaxed volume is given by the shaded area in Fig. 11.5b, it follows that the strain energy of the system in the presence of the crack is given by

$$U_{\text{strain}} = U_0 + \frac{V_0 \sigma_{\text{app}}^2}{2Y} - \frac{\sigma_{\text{app}}^2}{2Y} \left[\frac{\pi c^2 t}{2} \right] \quad (11.5)$$

where t is the thickness of the plate. The third term represents the *strain energy released* in the relaxed volume.

¹⁸⁴ When a bond is stretched, energy is stored in that bond in the form of elastic energy. This energy can be converted to other forms of energy as any schoolboy with a slingshot can attest; the elastic energy stored in the rubber band is converted into kinetic energy of the projectile. If by chance a pane of glass comes in the way of the projectile, that kinetic energy will in turn be converted to other forms of energy such as thermal, acoustic, and surface energy. In other words, the glass will shatter and some of the kinetic energy will have created new surfaces.

Surface energy

To form a crack of length c , an energy expenditure of

$$U_{\text{surf}} = 2\gamma ct \tag{11.6}$$

is required, where γ is the intrinsic surface energy of the material. The factor 2 arises because two (bottom and top) new surfaces are created by the fracture event.

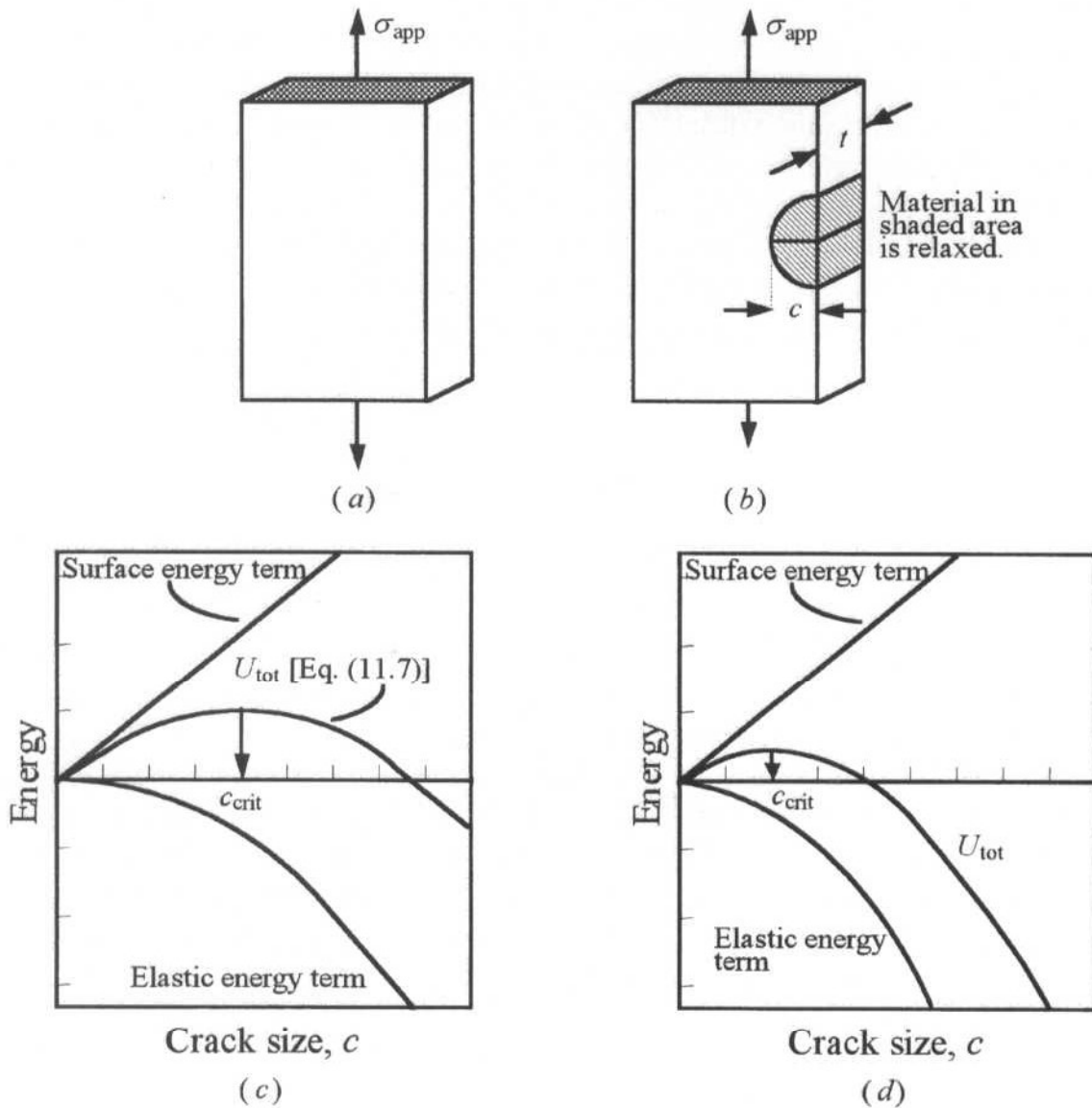


Figure 11.5 (a) Uniformly stressed solid. (b) Relaxed volume in vicinity of crack of length c . (c) Plot of Eq. (11.7) as a function of c . The top curve represents the surface energy term, and the lower curve represents the strain energy release term. Curve labeled U_{tot} is sum of the two curves. The critical crack length c_{crit} at which fast fracture will occur corresponds to the maximum. (d) Plot of Eq. (11.7) on the same scale as in part (c) but for $\sqrt{2}$ times the applied stress applied in (c). Increasing the applied stress by that factor reduces c_{crit} by a factor of 2.

The total energy change of the system upon introduction of the crack is simply the sum of Eqs. (11.5) and (11.6), or

$$U_{\text{tot}} = U_0 + \frac{V_0 \sigma_{\text{app}}^2}{2Y} - \frac{\sigma_{\text{app}}^2}{2Y} \left[\frac{\pi c^2 t}{2} \right] + 2\gamma ct \quad (11.7)$$

Since the surface energy term scales with c and the strain energy term scales with c^2 , U_{tot} has to go through a *maximum* at a certain critical crack size c_{crit} (Fig. 11.5c). This is an important result since it implies that extending a crack that is smaller than c_{crit} *consumes rather than liberates energy and is thus stable*. In contrast, *flaws that are longer than c_{crit} are unstable since extending them releases more energy than is consumed*. Note that increasing the applied stress (Fig. 11.5d) will result in failure at smaller critical flaw sizes. For instance, a solid for which the size of the largest¹⁸⁵ flaw lies somewhere between those shown in Fig. 11.5c and d will *not* fail at the stress shown in Fig. 11.5c, but will fail if that stress is increased (Fig. 11.5d).

The location of the maximum is determined by differentiating Eq. (11.7) and equating it to zero. Carrying out the differentiation, replacing σ_{app} by σ_f , and rearranging terms, one can show that the condition for failure is

$$\sigma_f \sqrt{\pi c_{\text{crit}}} = 2\sqrt{\gamma Y} \quad (11.8)$$

A more exact calculation yields

$$\boxed{\sigma_f \sqrt{\pi c_{\text{crit}}} \geq \sqrt{2\gamma Y}} \quad (11.9)$$

and is the expression used in subsequent discussions.¹⁸⁶ This equation predicts that a critical combination of *applied stress and flaw size is required to cause failure*. The combination $\sigma\sqrt{\pi c}$ occurs so often in discussing fast fracture that it is abbreviated to a single symbol K_I with units $\text{MPa} \cdot \text{m}^{1/2}$, and is referred to as the **stress intensity factor**. Similarly, the combination of terms on the right-hand side of Eq. (11.9), sometimes referred to as the **critical stress intensity factor**, or more commonly the **fracture toughness**, is abbreviated by the symbol K_{Ic} . Given these abbreviations, the condition for fracture can be succinctly rewritten as

$$\boxed{K_I \geq K_{Ic}} \quad (11.10)$$

Equations (11.9) and (11.10) were derived with the implicit assumption that the only factor keeping the crack from extending was the creation of new

¹⁸⁵ The largest flaw is typically the one that will cause failure, since it becomes critical before other smaller flaws (see Fig. 11.8a).

¹⁸⁶ Comparing Eqs. (11.8) and (11.9) shows that the estimate of the volume over which the stress is relieved in Fig. 11.5b was off by a factor of $\sqrt{2}$, which is not too bad.

Table 11.1 Data for Young's modulus Y , Poisson's ratio, and K_{Ic} values of selected ceramics at ambient temperatures[†]

	Y , (GPa)	Poisson's ratio	K_{Ic} , MPa · m ^{1/2}	Vickers hardness, GPa
Oxides				
Al ₂ O ₃	390	0.20–0.25	2.0–6.0	19.0–26.0
Al ₂ O ₃ (single crystal, 10 $\bar{1}2$)	340		2.2	
Al ₂ O ₃ (single crystal, 0001)	460		>6.0	
BaTiO ₃	125			
BeO	386	0.34		0.8–1.2
HfO ₂ (monoclinic)	240			
MgO	250–300	0.18	2.5	6.0–10.0
MgTi ₂ O ₅	250			
MgAl ₂ O ₄	248–270		1.9–2.4	14.0–18.0
Mullite [fully dense]	230	0.24	2.0–4.0	15.0
Nb ₂ O ₅	180			
PbTiO ₃	81			
SiO ₂ (quartz)	94	0.17		12.0 (011)
SnO ₂	263	0.29		
TiO ₂	282–300			10.0 ± 1.0
ThO ₂	250		1.6	10.0
Y ₂ O ₃	175		1.5	7.0–9.0
Y ₃ Al ₅ O ₁₂				18.0 ± 1.0
ZnO	124			2.3 ± 1.0
ZrSiO ₄ (zircon)	195	0.25		≈15.0
ZrO ₂ (cubic)	220	0.31	3.0–3.6	12.0–15.0
ZrO ₂ (partially stabilized)	190	0.30	3.0–15.0	13.0
Carbides, Borides, and Nitrides and Silicides				
AlN	308	0.25		12.0
B ₄ C	417–450	0.17		30.0–38.0
BN	675			
Diamond	1000			
MoSi ₂	400			
Si	107	0.27		10.0
SiC [hot pressed]	440 ± 10	0.19	3.0–6.0	26.0–36.0
SiC (single crystal)	460		3.7	
Si ₃ N ₄ Hot Pressed (dense)	300–330	0.22	3.0–10.0	17.0–30.0
TiB ₂	500–570	0.11		18.0–34.0
TiC	456	0.18	3.0–5.0	16.0–28.0
WC	450–650		6.0–20.0	
ZrB ₂	440	0.14		22.0
Halides and Sulfides				
CaF ₂	110		0.80	1.800
KCl (forged single crystal)	24		≈0.35	0.120

Table 11.1 Continued

	Y , (GPa)	Poisson's ratio	K_{Ic} , $\text{MPa} \cdot \text{m}^{1/2}$	Vickers hardness, GPa
MgF_2	138		1.00	6.000
SrF_2	88		1.00	1.400
Glasses and Glass Ceramics				
Aluminosilicate (Corning 1720)	89	0.24	0.96	6.6
Borosilicate (Corning 7740)	63	0.20	0.75	6.5
Borosilicate (Corning 7052)	57	0.22		
LAS (glass-ceramic)	100	0.30	2.00	
Silica (fused)	72	0.16	0.80	6.0–9.0
Silica (96%)	66		0.70	
Soda Lime Silica Glass	69	0.25	0.82	5.5

[†] The fracture toughness is a function of microstructure. The values given here are mostly for comparison's sake.

surface. This is only true, however, for extremely brittle systems such as inorganic glasses. In general, however, when other energy dissipating mechanisms, such a plastic deformation at the crack tip, are operative, K_{Ic} is defined as

$$K_{Ic} = \sqrt{YG_c} \quad (11.11)$$

where G_c is the **toughness** of the material in joules per square meter. For purely brittle solids,¹⁸⁷ the toughness approaches the limit $G_c = 2\gamma$. Table 11.1 lists Young's modulus, Poisson's ratio, and K_{Ic} values of a number of ceramic materials. It should be pointed out that since (see below) K_{Ic} is a material property that is also microstructure-dependent, the values listed in Table 11.1 are to be used with care.

Finally it is worth noting that the Griffith approach, Eq. (11.10), can be reconciled with Eq. (11.2) by assuming that ρ is on the order of $10r_0$, where r_0 is the equilibrium interionic distance (see Prob. 11.3). In other words, the Griffith approach implicitly assumes that the flaws are atomically sharp, a fact that must be borne in mind when one is experimentally determining K_{Ic} for a material.

To summarize: fast fracture will occur in a material when the product of the applied stress and the square root of the flaw dimension are comparable to that material's fracture toughness.

¹⁸⁷ Under these conditions, one may calculate the surface energy of a solid from a measurement of K_{Ic} (see the section on measuring surface energies in Chap. 4).

WORKED EXAMPLE 11.1

(a) A sharp edge notch 120 μm deep is introduced in a thin magnesia plate. The plate is then loaded in tension normal to the plane of the notch. If the applied stress is 150 MPa, will the plate survive? (b) Would your answer change if the notch were the same length but was as internal notch (Fig. 11.4b) instead of an edge notch?

Answer

(a) To determine whether the plate will survive the applied stress, the stress intensity at the crack tip needs to be calculated and compared to the fracture toughness of MgO, which according to Table 11.1 is $2.5 \text{ MPa} \cdot \text{m}^{1/2}$.

K_I in this case is given

$$K_I = \sigma\sqrt{\pi c} = 150\sqrt{3.14 \times 120 \times 10^{-6}} = 2.91 \text{ MPa} \cdot \text{m}^{1/2}$$

Since this value is greater than K_{Ic} for MgO, it follows that the plate will fail.

(b) In this case, because the notch is an internal one, it is not as detrimental as a surface or edge notch and

$$K_I = \sigma\sqrt{\pi \frac{c}{2}} = 150\sqrt{3.14 \times 60 \times 10^{-6}} = 2.06 \text{ MPa} \cdot \text{m}^{1/2}$$

Since this value is $< 2.5 \text{ MPa} \cdot \text{m}^{1/2}$ it follows that the plate would survive the applied load.

Before one explores the various strategies to increase the fracture toughness of ceramics, it is important to appreciate how K_{Ic} is measured.

Experimental Details: Measuring K_{Ic}

There are several techniques by which K_{Ic} can be measured. The two most common methods entail measuring the fracture stress for a given geometry and known initial crack length and measuring the lengths of cracks emanating from hardness indentations.

Fracture Stress

Equation (11.9) can be recast in its most general form

$$\Psi\sigma_{\text{frac}}\sqrt{\pi c} \geq K_{Ic} \quad (11.12)$$

where Ψ is a dimensionless constant on the order of unity that depends on the sample shape, the crack geometry, and its relative size to the sample dimensions. This relationship suggests that to measure K_{Ic} , one would start with an *atomically* sharp crack [an implicit assumption made in deriving Eq. (11.10) — see Prob. 11.3] of length c and measure the stress at which fracture occurs. Given

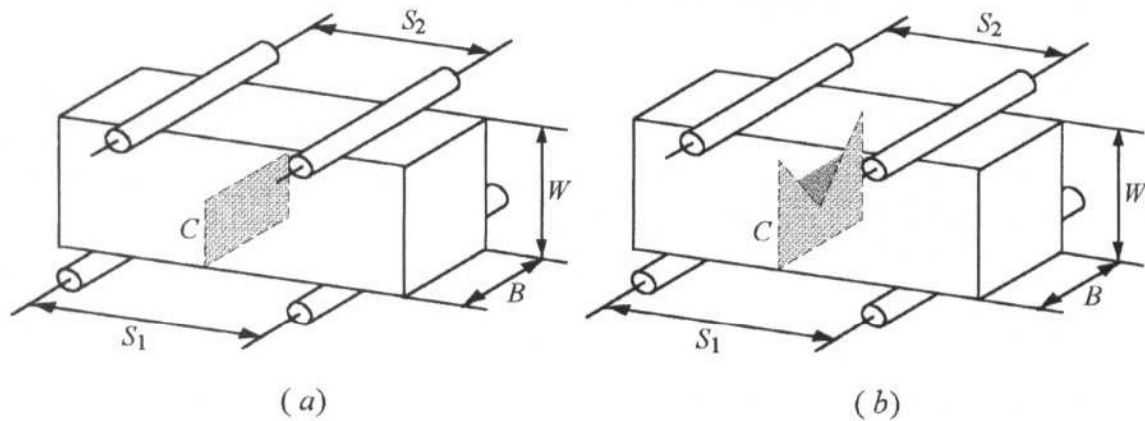


Figure 11.6 (a) Schematic of single-edge notched beam specimen; (b) Chevron notch specimen.

the sample and crack geometries, Ψ can be looked up in various fracture mechanics handbooks, and then K_{Ic} is calculated from Eq. (11.12). Thus, in principle, it would appear that measuring K_{Ic} is fairly straightforward; experimentally, however, the difficulty lies in introducing an atomically sharp crack.

Two of the more common test configurations are shown in Fig. 11.6. A third geometry not shown here is the **double torsion test**, which in addition to measuring K_{Ic} can be used to measure crack velocity versus K curves. This test is described in greater detail in the next chapter.

Single-edge notched beam (SENB) test

In this test a notch of initial depth c is introduced, usually by using a diamond wheel, on the tensile side of a flexure specimen (Fig. 11.6a). The sample is loaded until failure, and c is taken as the initial crack length. Fracture toughness K_{Ic} is calculated from

$$K_{Ic} = \frac{3\sqrt{c}(S_1 - S_2)\xi F_{\text{fail}}}{2BW^2}$$

where F_{fail} is the load at which the specimen failed and ξ is a calibration factor. The other symbols are defined in Fig. 11.6a. The advantage of this test lies in its simplicity — its major drawback, however, is that the condition that the crack be atomically sharp is, more often than not, unfulfilled, which causes one to overestimate K_{Ic} .

Chevron notch (CN) specimen¹⁸⁸

In this configuration, shown schematically in Fig. 11.6b, the chevron notch specimen looks quite similar to the SENB except for the vital difference that the shape of the initial crack is not flat but chevron-shaped, as shown by the shaded area. The constant widening of the crack front as it advances causes

¹⁸⁸ A *chevron* is a figure or a pattern having the shape of a V.

crack growth to be stable *prior* to failure. Since an increased load is required to continue crack extension, it is possible to create an atomically sharp crack in the specimen *before* final failure, which eliminates the need to precrack the specimen. The fracture toughness¹⁸⁹ is then related to the maximum load at fracture F_{fail} and the minimum of a compliance function ξ^* .

$$K_{Ic} = \frac{(S_1 - S_2)\xi^* F_{\text{fail}}}{BW^{3/2}}$$

General remarks

Unless care is taken in carrying out the fracture toughness measurements, different tests will result in different values of K_{Ic} . There are three reasons for this: (1) The sample dimensions were too small, compared to the process zone (which is the zone ahead of the crack tip that is damaged). (2) The internal stresses generated during machining of the specimens were not sufficiently relaxed before the measurements were made. (3) The crack tip was not atomically sharp. As noted above, if the fracture initiating the flaw is not atomically sharp, apparently higher K_{Ic} values will be obtained. Thus although simple in principle, the measurement of K_{Ic} is fraught with pitfalls, and care must be taken if reliable and accurate data are to be obtained.

Hardness Indentation Method

Due to its simplicity, its nondestructive nature, and the fact that minimal machining is required to prepare the sample, the use of the Vickers hardness indentations to measure K_{Ic} has become quite popular. In this method, a diamond indenter is applied to the surface of the specimen to be tested. Upon removal, the sizes of the cracks that emanate (sometimes) from the edges of the indent are measured, and the Vickers hardness H in GPa of the material is calculated. A number of empirical and semiempirical relationships have been proposed relating K_{Ic} , c , Y , and H , and in general the expressions take the form

$$K_{Ic} = \Phi \sqrt{a} H \left(\frac{Y}{H} \right)^{0.4} f \left(\frac{c}{a} \right) \quad (11.13)$$

where Φ is a geometric constraint factor and c and a are defined in Fig. 11.7. The exact form of the expression used depends on the type of crack that emanates from the indent.¹⁹⁰ A cross-sectional view and a top view of the

¹⁸⁹ For more information, see J. Sung and P. Nicholson. *J. Amer. Cer. Soc.*, **72** (6):1033–1036 (1989).

¹⁹⁰ For more information, see G. R. Anstis, P. Chantikul, B. R. Lawn, and D. B. Marshall. *J. Amer. Cer. Soc.*, **64**:533 (1981), and R. Matsumoto, *J. Amer. Cer. Soc.*, **70**(C):366 (1987). See also Problem 11.9.

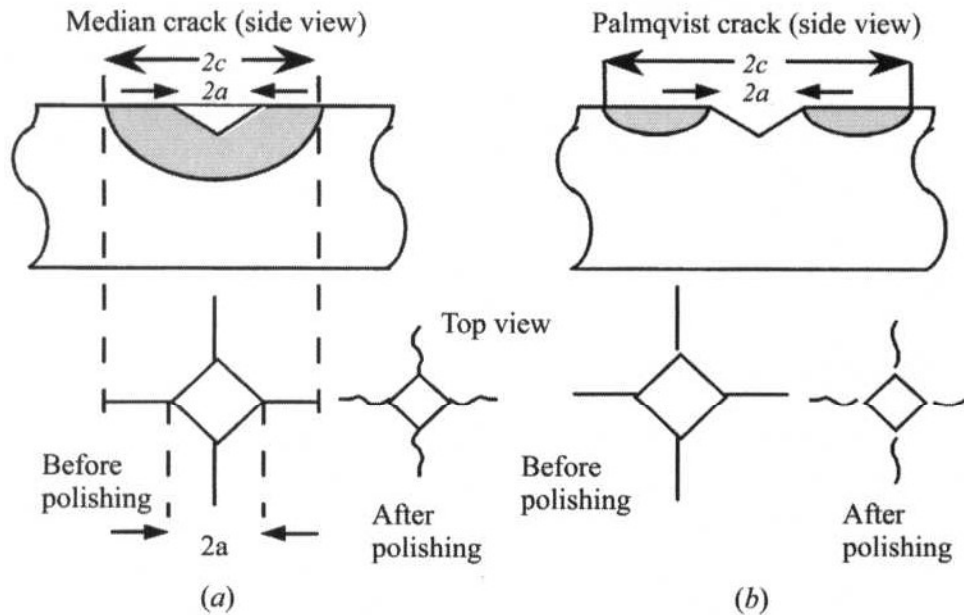


Figure 11.7 Crack systems developed from the Vickers indents. (a) Side and top views of a median crack. (b) Top and side views of a Palmqvist crack.

two most common types of cracks of interest are shown in Fig. 11.7. At low loads, Palmqvist cracks are favored, while at high loads fully developed median cracks result. A simple way to differentiate between the two types is to polish the surface layers away; the median crack system will always remain connected to the inverted pyramid of the indent while the Palmqvist will become detached, as shown in Fig. 11.7b.

It should be emphasized that the K_{Ic} values measured using this technique are usually not as precise as those from other more macroscopic tests.

11.2.3 Compressive and Other Failure Modes

Whereas it is now well established that tensile brittle failure usually propagates unstably when the stress intensity at the crack tip exceeds a critical value, the mechanics of compressive brittle fracture are more complex and not as well understood. Cracks in compression tend to propagate stably and twist out of their original orientation to propagate parallel to the compression axis, as shown in Fig. 11.8b. Fracture in this case is caused not by the unstable propagation of a single crack, as would be the case in tension (Fig. 11.8a), but by the slow extension and linking up of many cracks to form a crushed zone. Hence it is not the size of the largest crack that counts, but the size of the average crack c_{av} . The compressive stress to failure is still given by

$$\sigma_{fail} \approx Z \frac{K_{Ic}}{\sqrt{\pi c_{av}}} \quad (11.14)$$

but now Z is a constant on the order of 15.

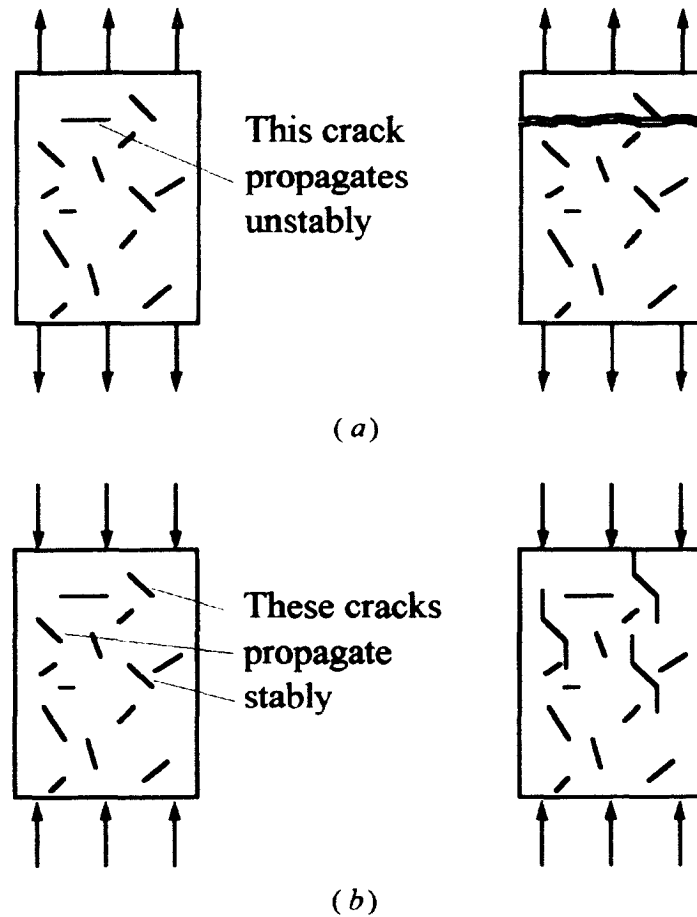


Figure 11.8 (a) Fracture in ceramics due to preexisting flaws tested in tension. Failure occurs by the unstable propagation of the worst crack that is also most favorably oriented. (b) During compressive loading, many cracks propagate stably, eventually linking up and creating a crush zone.¹⁹¹

Finally, in general there are three modes of failure, known as modes I, II, and III. Mode I (Fig. 11.9a) is the one that we have been dealing with so far. Modes II and III are shown in Fig. 11.9b and c, respectively. The same energy concepts that apply to mode I also apply to modes II and III. Mode I, however, is by far the more pertinent to crack propagation in brittle solids.

11.2.4 Atomistic Aspects of Fracture

Up to this point, the discussion has been mostly couched in macroscopic terms. Flaws were shown to concentrate the applied stress at their tip which ultimately led to failure. No distinction was made between brittle and ductile materials, and yet experience clearly indicates that the different classes of materials behave quite differently — after all, the consequences

¹⁹¹ Adapted from M. F. Ashby and D. R. Jones, *Engineering Materials*, vol. 2, Pergamon Press, New York, 1986.

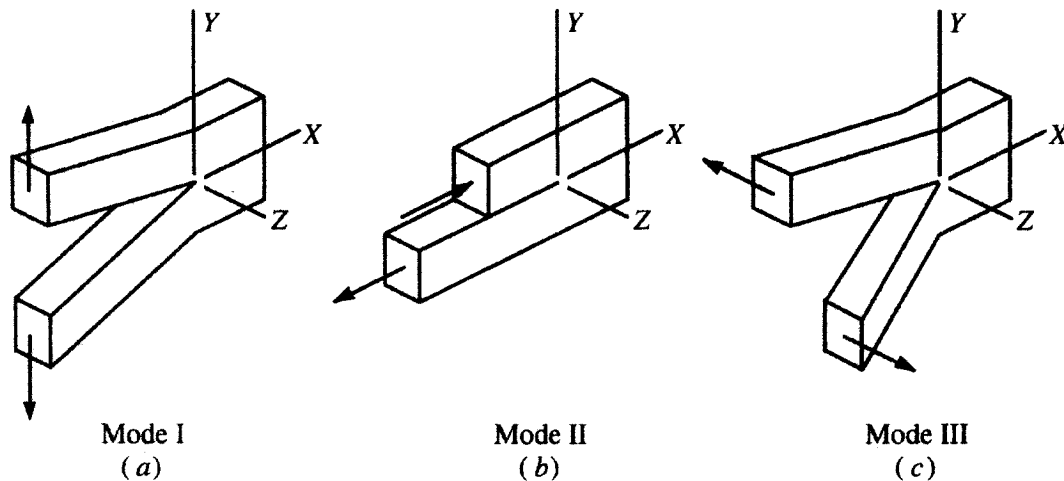


Figure 11.9 The three modes of failure: (a) opening mode, or mode I, characterized by K_{Ic} ; (b) sliding mode, or mode II, K_{IIc} ; (c) tearing mode, or mode III, K_{IIIc} .

of scribing a glass plate are quite different from those of a metal one. Thus the question is, what renders brittle solids notch-sensitive, or more directly, why are ceramics brittle?

The answer is related to the crack tip plasticity. In the foregoing discussion, it was assumed that intrinsically brittle fracture was free of crack-tip plasticity, i.e., dislocation generation and motion. Given that dislocations are generated and move under the influence of *shear stresses*, two limiting cases can be considered:

1. The cohesive tensile stress ($\approx Y/10$) is *smaller* than the cohesive strength in shear, in which case the solid can sustain a sharp crack and the Griffith approach is valid.
2. The cohesive tensile stress is *greater* than the cohesive strength in shear, in which case shear breakdown will occur (i.e., dislocations will move away from the crack tip) and the crack will lose its atomic sharpness. In other words, the emission of dislocations from the crack tip, as shown in Fig. 11.10a, will move material away from the crack tip, absorbing energy and causing crack blunting, as shown in Fig. 11.10b.

Theoretical calculations have shown that the ratio of theoretical shear strength to tensile strength diminishes as one proceeds from covalent to ionic to metallic bonds. For metals, the intrinsic shear strength is so low that flow at ambient temperatures is almost inevitable. Conversely, for covalent materials such as diamond and SiC, the opposite is true: the exceptionally rigid tetrahedral bonds would rather extend in a mode I type of crack than shear.

Theoretically, the situation for ionic solids is less straightforward, but direct observations of crack tips in transmission electron microscopy tend to support the notion that most covalent and ionic solids are truly

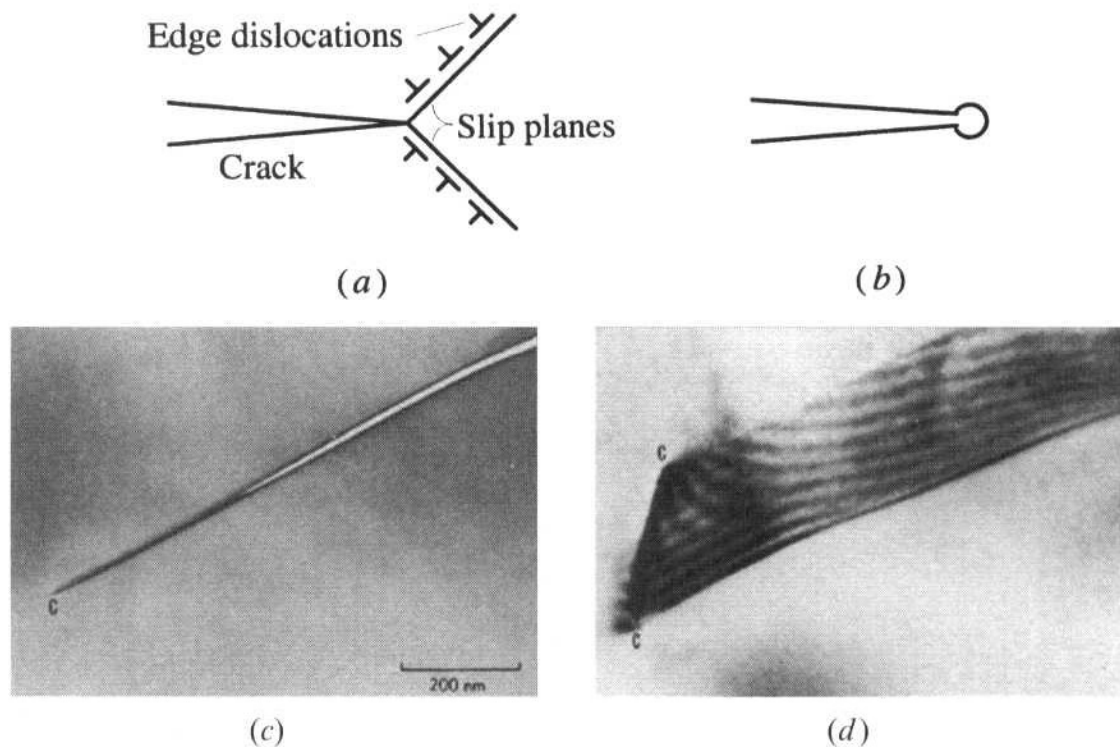


Figure 11.10 (a) Emission of dislocations from crack tip. (b) Blunting of crack tip due to dislocation motion. (c) Transmission electron micrograph of cracks in Si at 25°C. (d) Another crack in Si formed at 500°C, where dislocation activity in vicinity of crack tip is evident.¹⁹²

brittle at room temperature (see Fig. 11.10c). Note that the roughly order-of-magnitude difference between the fracture toughness of metals (20 to 100 MPa·m^{1/2}) and ceramics is directly related to the lack of crack-tip plasticity in the latter — moving dislocations consumes quite a bit of energy.

The situation is quite different at higher temperatures. Since dislocation mobility is thermally activated, increasing the temperature will tend to favor dislocation activity, as shown in Fig. 11.10d, which in turn increases the ductility of the material. Thus the condition for brittleness can be restated as follows: Solids are brittle when the energy barrier for dislocation motion is large relative to the thermal energy kT available to the system. Given the large flow stresses required to move dislocations at elevated temperatures in oxide single crystals (Fig. 11.11), it is once again not surprising that ceramics are brittle at room temperatures. Finally, note that dislocation activity is not the only mechanism for crack blunting. At temperatures above the glass transition temperature viscous flow is also very effective in blunting cracks.

¹⁹² B. R. Lawn, B. J. Hockey, and S. M. Wiederhorn, *J. Mat. Sci.*, **15**:1207 (1980). Reprinted with permission.

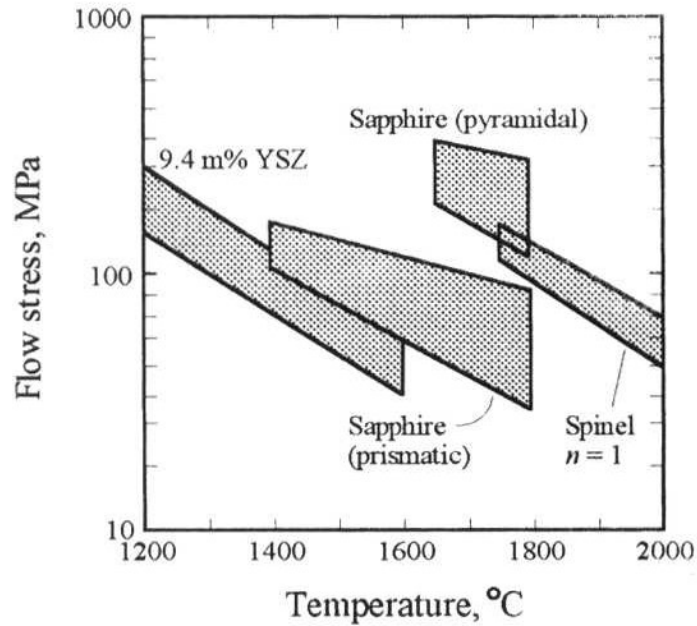


Figure 11.11 Temperature dependence of flow stress for yttria-stabilized zirconia (YSZ), sapphire, and equimolar spinel.¹⁹³

11.3 Strength of Ceramics

Most forming methods that are commonly used in the metal and polymer industries are not applicable for ceramics. Their brittleness precludes deformation methods; and their high melting points, and in some cases (e.g., Si_3N_4 , SiC) decomposition prior to melting, preclude casting. Consequently, as discussed in the previous chapter, most polycrystalline ceramics are fabricated by either solid- or liquid-phase sintering, which can lead to flaws. For example, how agglomeration and inhomogeneous packing during powder preparation often led to the development of flaws in the sintered body was discussed in Chap. 10. Inevitably, flaws are always present in ceramics. In this section, the various types of flaws that form during processing and their effect on strength are discussed. The subsequent section deals with the effect of grain size on strength, while Sec. 11.3.3 deals briefly with strengthening ceramics by the introduction of compressive surface layers. Before one proceeds much further, however, it is important to briefly review how the strength of a ceramic is measured.

Experimental Details: Modulus of Rupture

Tensile testing of ceramics is time-consuming and expensive because of the difficulty in machining test specimens. Instead, the simpler transverse bending or flexure test is used, where the specimen is loaded to failure in either

¹⁹³ A. H. Heuer, cited in R. Raj, *J. Amer. Cer. Soc.*, **76**:2147–2174 (1993).